



Open Access

ORIGINAL ARTICLE

Male Endocrinology

# Androgen receptor deficiency in monocytes/macrophages does not alter adiposity or glucose homeostasis in male mice

Katya B Rubinow<sup>1</sup>, Barbara Houston<sup>1</sup>, Shari Wang<sup>1</sup>, Leela Goodspeed<sup>1</sup>, Kayoko Ogimoto<sup>1</sup>, Gregory J Morton<sup>1</sup>, Christopher McCarty<sup>2</sup>, Robert E Braun<sup>2</sup>, Stephanie T Page<sup>1</sup>

Androgen deprivation in men leads to increased adiposity, but the mechanisms underlying androgen regulation of fat mass have not been fully defined. Androgen receptor (AR) is expressed in monocytes/macrophages, which are resident in key metabolic tissues and influence energy metabolism in surrounding cells. Male mice bearing a cell-specific knockout of the AR in monocytes/macrophages (M-ARKO) were generated to determine whether selective loss of androgen signaling in these cells would lead to altered body composition. Wild-type (WT) and M-ARKO mice (12–22 weeks of age,  $n = 12$  per group) were maintained on a regular chow diet for 8 weeks and then switched to a high-fat diet for 8 additional weeks. At baseline and on both the regular chow and high-fat diets, no differences in lean mass or fat mass were observed between groups. Consistent with the absence of differential body weight or adiposity, no differences in food intake ( $3.0 \pm 0.5$  g per day for WT mice vs  $2.8 \pm 0.4$  g per day for M-ARKO mice) or total energy expenditure ( $0.6 \pm 0.1$  Kcal  $h^{-1}$  for WT mice vs  $0.5 \pm 0.1$  Kcal  $h^{-1}$  for M-ARKO mice) were evident between groups during high-fat feeding. Liver weight was greater in M-ARKO than that in WT mice ( $1.5 \pm 0.1$  g vs  $1.3 \pm 0.0$  g, respectively,  $P = 0.02$ ). Finally, M-ARKO mice did not exhibit impairments in glucose tolerance or insulin sensitivity relative to WT mice at any study time point. In aggregate, these findings suggest that AR signaling specifically in monocytes/macrophages does not contribute to the regulation of systemic energy balance, adiposity, or insulin sensitivity in male mice.

*Asian Journal of Andrology* (2018) 20, 276–283; doi: 10.4103/aja.aja\_54\_17; published online: 5 December 2017

**Keywords:** androgen receptor; knockout mice; macrophages; male hypogonadism; metabolic syndrome

## INTRODUCTION

Sufficient androgen exposure is important for maintaining metabolic health in men. Both physiologic and pharmacologic androgen deprivation in men lead to increases in fat mass with attendant risks of insulin resistance and type 2 diabetes mellitus.<sup>1–3</sup> The metabolic sequela of hypogonadism have broad clinical relevance given the high prevalence of late-onset hypogonadism among older men as well as the widespread use of androgen deprivation therapy in men with prostate cancer.<sup>4–7</sup> Androgen receptor (AR) is widely expressed in key metabolic tissues including liver, skeletal muscle, brain, and adipose tissue, but the specific mechanisms and critical cell types through which androgens regulate adiposity in men have not been fully defined.

Mechanistic insight into androgen-mediated regulation of fat mass may be gained from animal models. In parallel with hypogonadal men, male mice with global AR deficiency developed obesity with advancing age,<sup>8</sup> and androgen deprivation generated either through orchietomy or global AR deletion conferred increased adiposity and worsened glucose tolerance in male mice on a high-fat diet.<sup>9</sup> Interestingly, this phenotype of increased adiposity was not reproduced with selective AR deletion in adipocytes, hepatocytes, or skeletal muscle in male mice

on a regular chow diet.<sup>10–12</sup> Within adipose tissue, AR is expressed in preadipocytes and mature adipocytes as well as in resident immune cell populations. Adipose tissue immune cells play critical roles in regulating energy metabolism, insulin sensitivity, and adipocyte function within adipose tissue;<sup>13–16</sup> thus, AR signaling in resident immune cells could contribute to androgen-mediated regulation of adiposity in men.

Previously, we have shown that AR deficiency in bone marrow-derived cells led to increased visceral fat mass in male mice on a regular chow diet.<sup>17</sup> AR is broadly expressed among immune cells present in adipose tissue including lymphocytes, macrophages, and neutrophils,<sup>18</sup> so the observed phenotype could have resulted from AR deletion in a number of hematopoietic cell types. Among these cell types, adipose tissue macrophages (ATMs) in particular have been implicated in the regulation of adipocyte differentiation, lipid and glucose metabolism, and adipokine secretion, as well as adipose tissue remodeling.<sup>13,19–23</sup> Androgen signaling in macrophages has demonstrated roles in key cellular functions including chemotaxis and cytokine secretion,<sup>18,24,25</sup> as illustrated by reduced tumor necrosis factor- $\alpha$  (TNF $\alpha$ ) and chemokine receptor expression in AR-deficient macrophages.<sup>26</sup> To determine the relative contribution

<sup>1</sup>Division of Metabolism, Endocrinology, and Nutrition, Department of Medicine, University of Washington School of Medicine, Seattle, WA 98195, USA; <sup>2</sup>Jackson Laboratory, Bar Harbor, ME 04609, USA.

Correspondence: Dr. KB Rubinow (rubinow@uw.edu)

Received: 01 June 2017; Accepted: 29 September 2017

of abrogated AR signaling in these cells to the increased fat mass evident in mice with AR deficiency in all bone marrow-derived cells, we investigated fat mass and energy metabolism in male mice with monocyte/macrophage-specific AR deficiency (M-ARKO mice).

## MATERIALS AND METHODS

### *Animals and study design*

Mice were generated at the Jackson Laboratory, Bar Harbor, Maine, USA. Male mice bearing a cell-specific knockout of the androgen receptor gene (*Ar*) in macrophages (M-ARKO), along with controls, were generated by employing two strains: B6.129S1-Ar<sup>tm2.1</sup>Reb/J (Jackson Lab JR # 018450) and B6.129P2-Lyz2<sup>tm1</sup>(cre)Ifo/J strain (Jackson Lab JR # 004781). The B6.129S1-Ar<sup>tm2.1</sup>Reb/J strain contains a conditional allele of the X-linked *Ar* gene, in which exon 1 is floxed.<sup>27</sup> Since we wished to disable the floxed *Ar* locus in macrophages, we also employed a Cre-bearing strain, B6.129P2-Lyz2<sup>tm1</sup>(cre)Ifo/J, in which Cre coding sequence, inserted into the first coding ATG site of the *Lyz2* gene, is under the control of this gene's promoter.<sup>28</sup> To generate the mice to be used for this project, successive matings were set up as follows. First, we generated males that were heterozygous for the *Lyz2*-Cre-bearing locus by mating B6.129P2-Lyz2<sup>tm1</sup>(cre)Ifo/J males homozygous for the *Lyz2*-Cre locus to C57BL/6J females. All of the offspring from this mating would be predicted to be heterozygous for the *Lyz2*-Cre locus. In a second set of matings, the resultant males that were heterozygous for *Lyz2*-Cre were mated to B6.129S1-Ar<sup>tm2.1</sup>Reb/J females homozygous for the X-linked *Ar*tm2.1 floxed allele. Male offspring from this second set of matings would all be predicted to be hemizygous for the *Ar*tm2.1 floxed allele, and either heterozygous for the *Lyz2*-Cre allele or homozygous for the *Lyz2* wild-type (WT) allele. Males hemizygous for the X-linked *Ar*tm2.1 floxed allele and hemizygous for the *Lyz2*-Cre allele would be designated as having the genotype X\_*Ar*tm2.1\_FL/Y; *Lyz2*-Cre/*Lyz2*. Due to their bearing a *Lyz2*-Cre allele, mice with this genotype would be predicted to have the floxed *Ar*tm2.1 allele disabled in macrophages. Males hemizygous for the *Ar*tm2.1 allele and homozygous for the *Lyz2* WT allele would be predicted to have the genotype X\_*Ar*tm2.1\_FL/Y; *Lyz2*/*Lyz2*. Due to their lack of a Cre-modified allele, mice with this genotype would be predicted to have intact and therefore functional *Ar* allele in all their tissues. These would be designated as the controls. Mice of both genotypes would be generated within litters from the second set of matings, enabling generation of both M-ARKO males and control males. Females, which were also made from these matings, were not utilized.

Tail tips from phenotypic males obtained from the above matings were genotyped to determine whether the mice were M-ARKOs or controls as follows. To screen for the presence of the *Lyz2*-Cre allele, we utilized primers *Lyz2*\_66 (5' CCC AGA AAT GCC AGA TTA CG 3') and *Lyz2*\_67 (5' CTT GGG CTG CCA GAA TTT CTC 3'). These primers would yield an expected product size of ~700 bp if the *Lyz2*-Cre allele was present. Polymerase chain reaction (PCR) cycling conditions used to detect this allele utilized 1.5 mmol l<sup>-1</sup> MgCl<sub>2</sub> and 0.5 μmol l<sup>-1</sup> of each primer, with cycling conditions of: 95°C for 2 min; 35 cycles of 95°C for 30 s, 62°C for 1 min, 72°C for 1 min; and a final extension of 72°C for 2 min followed by a cooling step. We screened for both the 5' and 3' Lox P sites of the *Ar*tm2.1 allele. To assay for the 5' Lox P site, we used primers AD20 (5' CAG CAC CCT ACA CTA GAA TAC TG 3') and AD21 (5' AAT GAC CTG AGA GTG CTT CCT CC 3'). These primers would give an expected product side of ~250 bp for the floxed 5' site and ~205 bp for the corresponding WT allele that lacked the Lox P site. To test for the 3' Lox P site, we employed primers

AD 18 (5' AGG GCA CAG AGT AAG CAG TTT GC 3') and AD 19 (5' TCC AGA TGT AGG ACA GAC CTT CC 3'), which would give product sizes of ~200 bp if the 3' LoxP site was present and ~125 bp if this site was absent. PCR reactions contained 1.25 mmol l<sup>-1</sup> of MgCl<sub>2</sub> and 0.5 μmol l<sup>-1</sup> of each primer. Cycling conditions were: 95°C for 2 min; 35 cycles of 95°C for 30 s, 58°C for 30 s, 72°C for 30 min; and a final extension of 72°C for 5 min followed by a cooling step. These PCR products derived from both primer pairs were initially sequenced to ensure generation of expected sequences. As noted, males shown to bear the genotype X\_*Ar*tm2.1\_FL/Y; *Lyz2*-Cre/*Lyz2* were designated as M-ARKO. These mice were assumed to have the floxed *Ar* allele knocked out in macrophages. Male mice that were determined to have the genotype X\_*Ar*tm2.1\_FL/Y; *Lyz2*/*Lyz2* were designated as controls.

Adult male age-matched M-ARKO mice and their littermate controls (12–22 weeks old, *n* = 12 per group) were studied at baseline and were maintained on a regular chow diet until study week 8. After study week 8, animals were then switched to a high-fat diet with 45% of calories derived from fat (D12451 formula, Research Diets, Inc.; New Brunswick, NJ, USA) for additional 8 weeks. Body weight and food intake were measured weekly, and body composition and glucose and insulin tolerance tests were performed at baseline, study week 8, and study week 16. Mice were jointly housed with 2–5 animals per cage until study week 16, when animals were housed individually for 2 weeks prior to indirect calorimetry studies while being maintained on the high-fat diet. Animals were then sacrificed by cervical dislocation and exsanguination, and tissues were perfused with 10% phosphate-buffered saline prior to harvest. Tissues were snap-frozen in liquid nitrogen. All aspects of the study were approved by the University of Washington (UW) Institutional Animal Care and Use Committee (IACUC), USA.

### *Body composition assessment*

Body composition was measured at baseline, 8 weeks, and 16 weeks using quantitative magnetic resonance (QMR) spectroscopy through the UW Nutrition Obesity Research Center (NORC) Energy Balance Core.<sup>17,29</sup> To better characterize discrete fat depots, body composition also was measured at 8 and 16 weeks through fat-water imaging using a 3 Tesla MR system as previously described.<sup>17</sup> Imaging was performed through the UW NORC Metabolic Imaging Core on a subset of animals (*n* = 7 per group) and provided quantification of total, subcutaneous, and visceral fat volume. A single radiologist conducted all analyses and was blinded to animal group (WT vs M-ARKO).

### *Glucose homeostasis*

Insulin tolerance tests (ITT) and glucose tolerance tests (GTT) entailed intraperitoneal injection of glucose (1.5 g per kg body weight, 20% dextrose solution) or insulin (0.75 U per kg body weight), respectively, in 5-h fasted mice with measurement of blood glucose at baseline and 15, 30, 60, 90, and 120 min after injection. Blood glucose measurement was performed with a handheld glucose meter (Accu-Chek, Basel, Switzerland).

### *Hepatic lipid measurement and plasma analyses*

Lipids were extracted from liver using a modified Folch method.<sup>30</sup> Hepatic triglyceride and cholesterol levels were quantified by colorimetric assay.<sup>17,31</sup> Plasma insulin, leptin, and adiponectin concentration levels were determined at baseline, 8 weeks, and at sacrifice through enzyme-linked immunosorbent assay (ELISA; Millipore, Billerica, MA, USA) according to manufacturer's instructions.<sup>17</sup> Plasma interleukin-6 (IL-6) concentrations also were measured at study termination through a commercially available ELISA.

**Indirect calorimetry studies**

Mice were housed singly for 2 weeks prior to calorimetry studies for acclimation and then placed in metabolic cages housed within the UW NORC. Animals were weighed three times a week, and calorimetry studies were initiated only once all animals were weight stable. Indirect calorimetry analyses were performed as described in detail elsewhere<sup>32</sup> using a Promethion<sup>®</sup> computer-controlled system (Sable Systems, Las Vegas, NV, USA). Animals were maintained on the high-fat diet during calorimetry studies and had *ad libitum* access to food and water. Normal 12-h light and dark cycles were continued, and measurements were obtained over 3 dark and 2 light cycles. Physical activity was assessed through XYZ infrared beam arrays (BXYZ-R; Sable Systems, Las Vegas, NV, USA), with each activity count defined as consecutive beam breaks along the y-axes. Both oxygen (O<sub>2</sub>) consumption and carbon dioxide (CO<sub>2</sub>) production were measured over 1 min at 10-min intervals, and respiratory quotient was calculated as CO<sub>2</sub> production/O<sub>2</sub> consumption. Energy expenditure (EE) was quantified in Kcal per hour using the Weir equation:  $EE = 60 \times (0.003941 \times V[O_2] + 0.001106 \times V[CO_2])$ , where V[O<sub>2</sub>] is the volume of O<sub>2</sub> uptake and V[CO<sub>2</sub>] is the volume of CO<sub>2</sub> output.<sup>33</sup>

**Quantitative real-time PCR**

As previously described,<sup>17</sup> RNA was extracted from roughly 100 mg of liver, skeletal muscle, and inguinal and epididymal adipose tissue. Gene expression was normalized to the geometric mean of glyceraldehyde 3-phosphate dehydrogenase (*Gapdh*) and  $\beta$ 2-microglobulin for liver, the geometric mean of non-POU domain-containing octamer-binding

protein (*NonO*) and  $\beta$ 2-microglobulin for adipose tissue, and  $\beta$ -actin for skeletal muscle. Gene expression data were analyzed using the  $\Delta\Delta$ Ct method.<sup>17,34</sup>

**Statistical analyses**

Between-group differences were assessed through unpaired Student's *t*-test for all outcomes measured at a single time point. Time-by-group interactions were analyzed by repeated measures ANOVA (RM-ANOVA) for outcomes measured at multiple time points. Data were presented as mean  $\pm$  standard error in figures and mean  $\pm$  standard deviation in the text. All analyses were performed using GraphPad Prism 5.0 software (GraphPad Software, Inc; La Jolla, CA, USA) with a *P* value threshold of <0.05 for statistical significance.

**RESULTS****AR deficiency in myeloid cells does not alter body weight or adiposity in male mice**

At baseline, no differences in body weight were evident between the WT animals and those with M-ARKO. Body weight and body weight gain in both groups remained comparable during 8 weeks of regular chow feeding and 8 subsequent weeks of high-fat feeding (**Figure 1a** and **1b**). Moreover, as expected, body weight increased more in both WT and M-ARKO mice with exposure to the high-fat diet for 8 weeks relative to chow. However, these changes in body weight followed a similar pattern in both groups, and no significant differences in body weight between WT and M-ARKO mice were apparent at any time point during the study.

On both the chow and high-fat diets, no between-group differences in lean body mass were seen (**Figure 1c**). At baseline, fat mass as

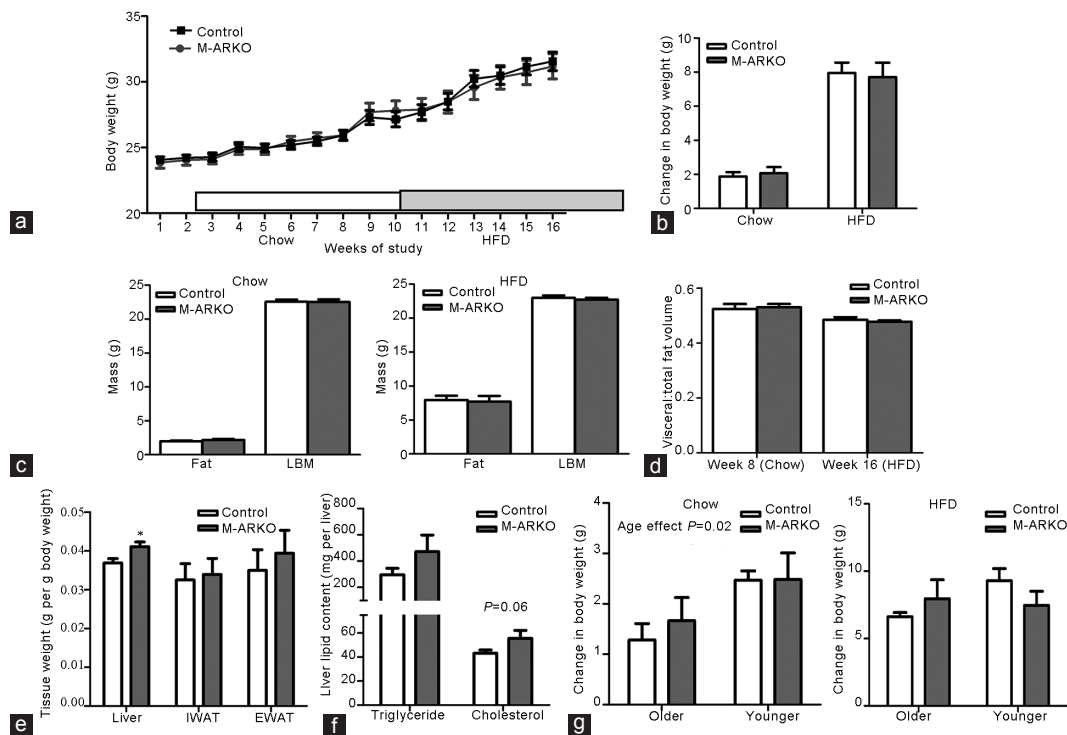


**Figure 1:** Body weight, body composition, and tissue weights over the study period. No differences in (a) absolute or (b) change in body weight were seen between M-ARKO and WT mice over the study period. (c) No significant differences in body composition were evident by QMR spectroscopy on either diet. (d) The ratios of visceral: total fat volume were similar in M-ARKO and WT mice on both regular chow diet and HFD. Livers from M-ARKO mice (e) weighed significantly more than those from WT animals and (f) had slightly more intrahepatic cholesterol content. (g) When mice were stratified by age, genotype did not significantly affect changes in body weight on either diet. EWAT: epididymal white adipose tissue; HFD: high-fat diet; IWAT: inguinal white adipose tissue; LBM: lean body mass; M-ARKO: myeloid-specific androgen receptor deficient; QMR: quantitative magnetic resonance; WT: wild-type. \**P* < 0.05.

assessed by QMR spectroscopy was identical in WT and M-ARKO animals (mean fat mass  $1.6 \pm 0.1$  g in both groups, data not shown), and fat mass remained similar between groups at study week 8 ( $2.2 \pm 0.1$  g in WT mice vs  $2.0 \pm 0.1$  g in M-ARKO mice). After study week 8, animals were transitioned to a high-fat diet with 45% of calories derived from fat in the form of lard. As expected, adiposity increased in both groups with 8 weeks of high-fat feeding relative to chow. At study week 16, fat mass remained comparable in WT and M-ARKO mice ( $8.0 \pm 0.6$  g vs  $7.7 \pm 0.8$  g, respectively). In parallel with QMR spectroscopy, fat-water imaging was employed to more sensitively quantify fat volume in both subcutaneous and visceral depots. Using this method, on both the regular chow and high-fat diets, the ratio of visceral to total fat volume did not differ between WT and M-ARKO mice (Figure 1d).

At sacrifice, after 8 weeks of high-fat feeding, both inguinal and epididymal fat pad weights were similar in WT and M-ARKO mice (Figure 1e). However, liver weight in M-ARKO mice was significantly albeit modestly greater than that in WT mice (mean liver weight  $1.5 \pm 0.1$  g in M-ARKO mice vs  $1.3 \pm 0.0$  g in WT mice,  $P = 0.02$ ). Total hepatic triglyceride content was not significantly different between groups ( $296.0 \pm 164.7$  mg for WT mice vs  $472.6 \pm 453.0$  mg for M-ARKO mice; Figure 1f), but greater hepatic cholesterol content in M-ARKO mice was seen as a statistical trend ( $43.2 \pm 9.0$  mg for WT mice vs  $55.6 \pm 23.9$  mg for M-ARKO mice,  $P = 0.06$ ).

On both the chow and high-fat diets, animals in both groups exhibited marked variability in body weight. Previously, global AR-deficient male mice were shown to develop age-dependent obesity,<sup>8</sup> suggesting that the variance in body weight among M-ARKO mice could be due to the wide age range of animals included in the study cohort. Accordingly, sensitivity analyses were performed to determine if an age-dependent effect of genotype was evident for change in body weight. Animals were grouped as older (date of birth: July 11, 2015–August 5, 2015) or younger (date of birth: August 30, 2015–September 21, 2015) with  $n = 6$  in each age group for both genotypes. Whereas younger mice appeared to gain more body weight on the chow diet, genotype did not affect body weight gain on either diet (Figure 1g).

#### M-ARKO mice do not exhibit impaired glucose tolerance or insulin sensitivity

We next determined whether M-ARKO mice exhibited alterations in glucose metabolism. While maintained on a chow diet, M-ARKO mice did not exhibit impairments in glucose tolerance or insulin sensitivity relative to WT mice (Figure 2a and 2b). Thus, neither the total nor incremental area under the glucose curve was different for either the GTT or ITT between groups.

As expected, after 8 weeks of high-fat feeding (study week 16), glucose tolerance worsened in both WT and M-ARKO animals relative to chow. However, fasting blood glucose levels were similar between groups. Although blood glucose levels at 30 min were lower in M-ARKO mice than in WT mice (Figure 2c), the total area under the glucose curve did not differ between groups. No significant differences were evident between groups in insulin sensitivity (Figure 2d), but M-ARKO mice had higher blood glucose levels during the late time points of the ITT. Fasting insulin levels were similar between groups on both the chow and high-fat diets (Figure 3a). As expected, following exposure to a high-fat diet for 8 weeks (study week 16), plasma insulin levels were elevated in both WT and M-ARKO mice relative to chow. However, neither significant time-by-group interactions nor between-group differences were found.

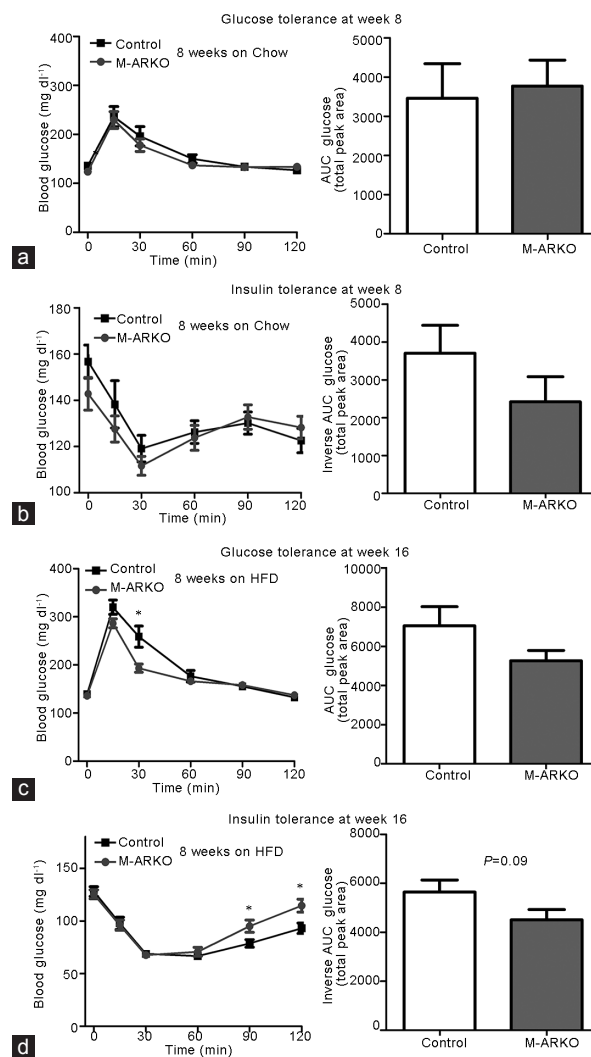


**Figure 2:** Glucose tolerance and insulin sensitivity on the chow diet and HFD. No differences in (a) glucose tolerance or (b) insulin sensitivity were evident after 8 weeks on a regular chow diet. After 8 weeks of high-fat feeding, (c) glucose tolerance and (d) insulin sensitivity remained similar between groups. HFD: high-fat diet; M-ARKO: myeloid-specific androgen receptor deficient; WT: wild-type. \* $P < 0.05$ .

#### Plasma cholesterol levels are lower in M-ARKO mice than that in WT controls

Over the course of the study period, no time-by-group interactions were apparent for plasma concentrations of leptin or adiponectin (Figure 3b and 3c, respectively). Serum leptin levels were higher in both groups after 8 weeks' exposure to the high-fat diet as expected given the increases in adiposity evident in both M-ARKO and WT mice. Plasma triglyceride levels also were similar between M-ARKO and WT mice on both diets (Figure 3d), but after 8 weeks on the high-fat diet (study week 16), M-ARKO mice exhibited lower plasma levels of total cholesterol relative to WT controls (mean cholesterol level:  $119.0 \pm 22.4$  mg dl<sup>-1</sup> for M-ARKO mice vs  $141.4 \pm 25.5$  mg dl<sup>-1</sup> for WT mice,  $P = 0.03$ ; Figure 3e). Circulating IL-6 levels did not differ between groups on either diet (Figure 3f).

#### M-ARKO and WT mice have similar EE and food intake

To further characterize the energy homeostasis phenotype of M-ARKO mice, measures of energy intake and EE were made using

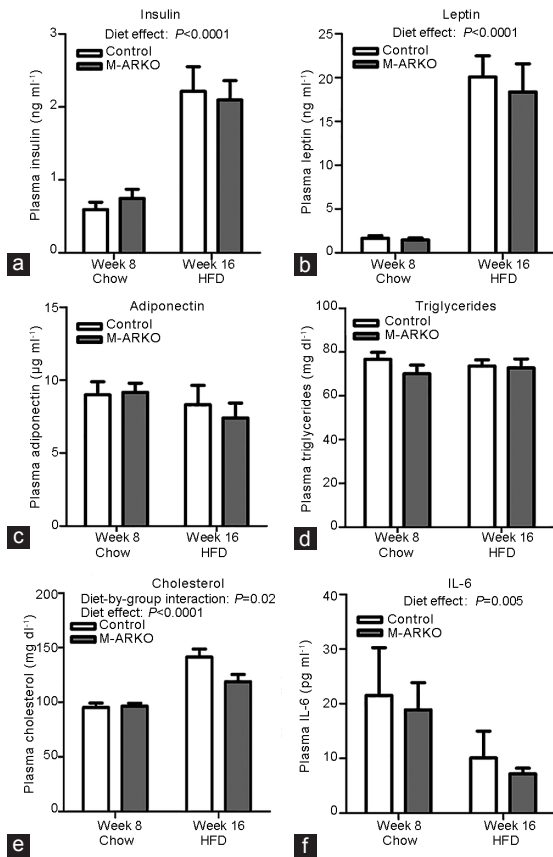


**Figure 3:** Plasma levels of insulin, adipokines, lipids, and IL-6. No time-by-group interactions were found for circulating levels of (a) insulin, (b) leptin, or (c) adiponectin, although significant diet effects were found for both insulin and leptin levels. (d) Plasma triglyceride levels were similar between groups on both diets, (e) but M-AR KO mice exhibited lower plasma cholesterol levels than WT mice at study week 16 (8 weeks on the HFD). (f) No differences in circulating IL-6 levels were evident between groups on either diet. HFD: high-fat diet; IL-6: interleukin-6; M-AR KO: myeloid-specific androgen receptor deficient; WT: wild-type.

indirect calorimetry after 8 weeks of high-fat feeding. There were no differences in food intake between the two groups (Figure 4a). Moreover, EE was similar in both groups ( $0.6 \pm 0.1$  Kcal  $h^{-1}$  for WT mice vs  $0.5 \pm 0.1$  Kcal  $h^{-1}$  for M-AR KO mice) and appeared comparable throughout both the light and dark cycles (Figure 4b). As both lean mass and fat mass have been shown to contribute to total EE,<sup>29</sup> we next performed regression analyses to examine the relationships between EE and both body weight and body composition. As expected, in WT mice, a positive correlation was found between EE and body weight, but this association was disrupted in M-AR KO mice (Figure 4c). Whereas WT mice also exhibited the expected positive association between EE and lean body mass, M-AR KO animals again showed a disrupted association (Figure 4d). No significant mean differences were found in either 24-h respiratory quotient (Figure 4e) or 24-h ambulatory activity (Figure 4f) between WT and M-AR KO mice, nor were differences found in these indices selectively during either the light or dark cycle (data not shown).

#### Expression of energy metabolism genes in peripheral metabolic tissues is similar in WT and M-AR KO mice

To gain additional insight into energy metabolism in M-AR KO mice, gene expression analyses were performed for key metabolic tissues

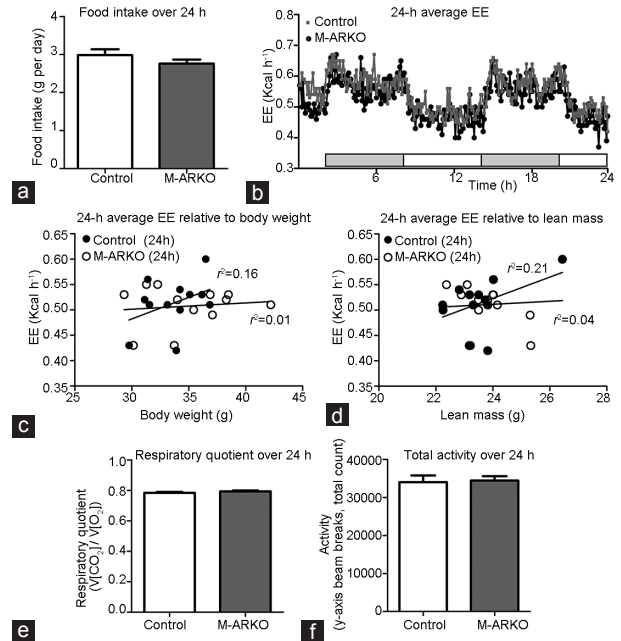


**Figure 4:** Indirect calorimetry findings on the high-fat diet. (a) No between-group differences were found in food intake. (b) Average energy expenditure did not differ between groups in either the dark cycle or the light cycle. (c) A positive association between body mass and 24-h average energy expenditure was evident in WT but not in M-AR KO mice. (d) Whereas a positive association also was seen between lean mass and 24-h average energy expenditure in WT mice, no association was seen in M-AR KO mice. No between-groups differences were found in (e) respiratory quotient and (f) ambulatory activity. Two data points for M-AR KO mice are wholly overlapping in (d), so only 11 data points appear. EE: energy expenditure; M-AR KO: myeloid-specific androgen receptor deficient; WT: wild-type;  $VIO_2$ : the volume of  $O_2$  uptake;  $VICO_2$ : the volume of  $CO_2$  output.

including skeletal muscle, liver, inguinal fat, and epididymal fat. In skeletal muscle, lower expression of phosphoglycerate kinase 1 (*Pgk1*) was found in M-AR KO mice (Figure 5a). No between-group differences in gene expression were found in either liver (Figure 5b) or epididymal fat (Figure 5c). In inguinal fat, M-AR KO mice exhibited slightly higher expression of the macrophage marker F4/80 (*Emr1*) (Figure 5d). Importantly, whole tissue AR (*Ar*) expression was ~15%–20% lower in M-AR KO mice relative to WT mice in liver (mean relative expression:  $1.2 \pm 0.3$  in M-AR KO mice vs  $1.4 \pm 0.3$  in WT mice,  $P = 0.15$ ) and epididymal fat (mean relative expression:  $0.8 \pm 0.2$  in M-AR KO mice vs  $1.0 \pm 0.2$  in WT mice,  $P = 0.10$ ), and differential *Ar* expression in inguinal fat was evident as a trend (mean relative expression:  $0.9 \pm 0.2$  in M-AR KO mice vs  $1.2 \pm 0.5$  in WT mice,  $P = 0.07$ ).

## DISCUSSION

Collectively, these findings demonstrate that monocyte/macrophage AR signaling does not substantially contribute to the regulation of body weight, adiposity, or insulin sensitivity in male mice. Body weight and body composition remained similar between WT and M-AR KO mice on both the regular chow and high-fat diets, and the relative volumes of visceral and subcutaneous fat also were unaffected by genotype on both diets. M-AR KO and WT mice exhibited comparable total EE and food intake, further arguing against a role for myeloid-specific AR in regulating systemic energy balance. Finally, no differences in glucose homeostasis were observed at any time point in the study, nor did gene expression profiles in key metabolic tissues differ between M-AR KO and WT mice.

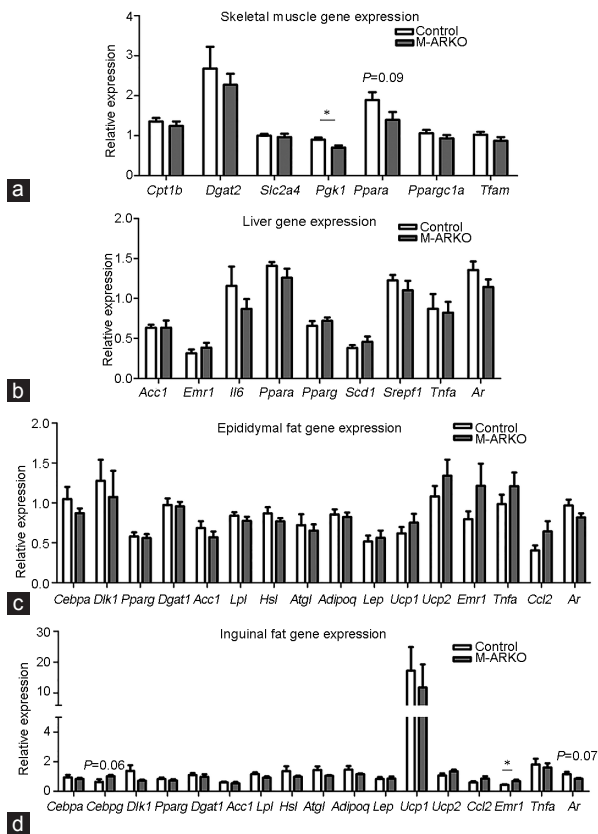


**Figure 5:** Gene expression in peripheral metabolic tissues. (a) Lower *Pgk1* expression in skeletal muscle was found in M-ARKO mice relative to WT controls. (b) Hepatic gene expression was similar in M-ARKO and WT mice. (c) No differences in epididymal fat gene expression were found between groups, (d) but M-ARKO mice exhibited higher *Emr1* expression than WT mice in inguinal fat. *Emr1*: EGF-like module-containing mucin-like hormone receptor-like 1; M-ARKO: myeloid-specific androgen receptor deficient; *Pgk1*: phosphoglycerate kinase 1; WT: wild-type. \* $P < 0.05$ .

Previously, we demonstrated that AR deficiency in hematopoietic cells led to increased visceral and total adiposity in male mice on a regular chow diet, with loss of differential adiposity after 8 weeks of high-fat feeding.<sup>17</sup> Further, we found differences in adipose tissue gene expression, hepatic lipid content, and circulating levels of adiponectin and IL-6. In the present study, only minimal differences in tissue gene expression were observed, and circulating markers did not differ between groups. Interestingly, plasma IL-6 levels tended to be lower across all animals on the high-fat diet relative to regular chow, a potentially surprising finding. Nevertheless, previous studies similarly have reported an absence of elevation or decrease in plasma IL-6 levels during high-fat feeding in mice.<sup>35,36</sup>

Our current study is not directly comparable to this previous study, as our prior study employed a bone marrow transplant model and a 60% high-fat diet. As the metabolic phenotype in our prior study was lost with prolonged high-fat feeding, we chose to use a lower fat diet with a shorter duration of high-fat feeding to reduce the likelihood of phenotypic differences between groups, becoming overwhelmed by the high-fat diet. Notably, loss of intact AR signaling has been shown to affect cellular phenotype in some but not all populations of myeloid cells, with a more prominent role in activated than resident monocytes.<sup>37</sup> The possibility therefore exists that the higher (60%) fat diet is necessary to elicit an activated monocyte/macrophage

phenotype that is influenced by AR signaling. However, despite these methodologic discrepancies, AR-deficient mice in both studies appeared more susceptible to hepatic lipid accumulation. In our bone marrow transplant study, hematopoietic AR deficiency led to increased intrahepatic cholesterol and triglyceride content, findings similar to the present study in which we observed greater liver weight and modestly more intrahepatic cholesterol in M-ARKO animals. The possibility exists that a more pronounced liver phenotype may have been reproduced in our current study if animals had been exposed to the 60% rather than the 45% high-fat diet.

M-ARKO mice did not exhibit impairments in glucose tolerance or insulin sensitivity at any time point. This finding is consistent with our previous study, which showed no impairment in insulin sensitivity despite increased visceral adiposity in animals with hematopoietic AR deficiency. Increased adiposity without impaired insulin sensitivity has been observed in other models of AR deficiency, as well.<sup>8,38</sup> In contrast, impaired insulin sensitivity has been identified in male mice with selective AR deficiency in hepatocytes and neurons.<sup>11,39</sup> Thus, aggregate findings to date suggest that respective AR-mediated effects on body composition and glucose regulation are conferred through discrete signaling effects in different cell types without a major contribution of myeloid cell-specific AR to either of them. In contrast, estrogen receptor- $\alpha$  deficiency in myeloid cells led to marked increases in both adiposity and insulin resistance in female mice.<sup>40</sup> Thus, our findings argue against a parallel role for AR signaling in myeloid cells as a principal determinant of fat mass or insulin sensitivity in males.

Indirect calorimetry findings showed no differences in EE between M-ARKO and WT mice. Unlike WT mice, M-ARKO animals did not exhibit the expected positive association between either body weight or lean mass and 24-h EE. The significance of this loss of association is unclear, though it is possible that the loss of a positive association between lean mass and EE could confer increased susceptibility to diet-induced obesity in M-ARKO mice over longer time frames. However, the differential association between lean mass and EE was largely due to a single outlier in the WT group. Therefore, future work could entail an extended study duration with inclusion of a larger number of animals to determine whether greater obesity may develop in M-ARKO mice with prolonged high-fat feeding. Notably, an interaction between AR deficiency and age has been observed in male mice with global AR deficiency.<sup>41</sup>

Lower expression of phosphoglycerate kinase 1 in skeletal muscle was seen in M-ARKO mice, as was a trend toward lower expression of PPAR $\alpha$ , findings consistent with reduced glycolysis and fatty acid  $\beta$ -oxidation, respectively. However, given the absence of differences between groups in fasting glucose levels, glucose tolerance, EE, or adiposity, the significance of these nominal differences in gene expression is unclear.

M-ARKO animals exhibited lower plasma total cholesterol levels and slightly higher intrahepatic cholesterol, though the latter finding did not achieve statistical significance. These findings add to a growing body of evidence supporting a potential role of monocyte/macrophage AR in systemic cholesterol metabolism. Previously, the nonaromatizable androgen dihydrotestosterone (DHT) was shown to inhibit cholesterol uptake by cultured macrophages in AR-dependent fashion.<sup>42</sup> More recently, AR signaling in monocytes/macrophages was shown to play important pathogenic roles in animal models of both atherosclerosis and aortic aneurysm development, with stronger contributory roles than either endothelial cells or smooth muscle cells.<sup>43,44</sup> Thus, both protective and harmful roles for AR signaling

in monocytes/macrophages have been postulated with regard to cholesterol metabolism, atherogenesis, and cardiovascular disease.

A primary limitation of our study is the heterogeneity evident in body weight, particularly among M-ARKO mice. This variability was likely resulted from the fairly wide age range of mice included in the study and could have obscured age-dependent changes in the metabolic phenotype of M-ARKO mice. Similarly, the time of exposure to each diet was only 8 weeks, and we cannot exclude the possibility that differences would have emerged with a longer study duration. However, our study benefitted from extensive metabolic phenotyping, including two discrete methods of assessing body composition as well as indirect calorimetry, and resultant data therefore argue strongly against a significant metabolic phenotype for M-ARKO mice. Finally, another possible limitation of our work is that *Lys2* may be lower in certain macrophage subsets;<sup>45</sup> therefore, AR deletion may not have been complete across macrophages of all activated phenotypes. Importantly, whole tissue gene expression analyses demonstrate reduced AR expression in metabolic tissues in M-ARKO mice. However, we cannot exclude the possibility that incomplete knockdown of AR expression was achieved and may account for the null findings in the present study. Therefore, a critical future step will be replication of these findings with careful quantification of AR expression specifically in macrophages resident within key metabolic tissues.

Collectively, our findings indicate that AR signaling in monocytes/macrophages is not a primary determinant of energy balance, body composition, or insulin sensitivity in male mice, though myeloid-specific AR may play a modest role in systemic cholesterol metabolism. The possibility exists that myeloid AR deficiency could produce a metabolic phenotype in male mice with more prolonged high-fat feeding or exposure to a higher fat diet. A potential metabolic role for myeloid AR signaling in females will also be the subject of future research. Thus, these findings suggest that diminished AR signaling in myeloid cells is unlikely to be a key determinant of the increased adiposity and associated metabolic risk evident among hypogonadal men.

## AUTHOR CONTRIBUTIONS

KBR contributed to the study design and performance, analyzed the data, and drafted the manuscript. BH, SW, and LG performed the research. KO and GJM performed the research and contributed to drafting the manuscript. REB and CM generated and provided the animals. STP contributed to the study conception and design and provided funding for the research. All authors read and approved the final manuscript.

## COMPETING INTERESTS

All authors declare no competing interests.

## ACKNOWLEDGMENTS

This work was funded by a University of Washington Diabetes Research Center New Investigator Award (P30 DK017047, for KBR), the Eunice Kennedy Shriver National Institute of Child Health and Development (6K12 HD053984, for KBR), National Institute of Diabetes and Digestive and Kidney Diseases (DK089056, for GJM and KO), the Eunice Kennedy Shriver National Institute of Child Health and Development (HD042454, for REB and STP), and the University of Washington Robert B McMillen Professorship in Lipid Research (for STP).

## REFERENCES

- 1 Bhasin S, Woodhouse L, Storer TW. Androgen effects on body composition. *Growth Horm IGF Res* 2003; 13: S63–71.
- 2 Finkelstein JS, Lee H, Burnett-Bowie SA, Pallais JC, Yu EW, *et al*. Gonadal steroids

and body composition, strength, and sexual function in men. *N Engl J Med* 2013; 369: 1011–22.

- 3 Derweesh IH, Diblasio CJ, Kincade MC, Malcolm JB, Lamar KD, *et al*. Risk of new-onset diabetes mellitus and worsening glycaemic variables for established diabetes in men undergoing androgen-deprivation therapy for prostate cancer. *BJU Int* 2007; 100: 1060–5.
- 4 Mulligan T, Frick MF, Zuraw QC, Stenhagen A, McWhirter C. Prevalence of hypogonadism in males aged at least 45 years: the HIM study. *Int J Clin Pract* 2006; 60: 762–9.
- 5 Araujo AB, O'Donnell AB, Brambilla DJ, Simpson WB, Longcope C, *et al*. Prevalence and incidence of androgen deficiency in middle-aged and older men: estimates from the Massachusetts male aging study. *J Clin Endocrinol Metab* 2004; 89: 5920–6.
- 6 Shahani S, Braga-Basaria M, Basaria S. Androgen deprivation therapy in prostate cancer and metabolic risk for atherosclerosis. *J Clin Endocrinol Metab* 2008; 93: 2042–9.
- 7 Cannata DH, Kirschenbaum A, Levine AC. Androgen deprivation therapy as primary treatment for prostate cancer. *J Clin Endocrinol Metab* 2012; 97: 360–5.
- 8 Fan W, Yanase T, Nomura M, Okabe T, Goto K, *et al*. Androgen receptor null male mice develop late-onset obesity caused by decreased energy expenditure and lipolytic activity but show normal insulin sensitivity with high adiponectin secretion. *Diabetes* 2005; 54: 1000–8.
- 9 Dubois V, Laurent MR, Jardi F, Antonio L, Lemaire K, *et al*. Androgen deficiency exacerbates high fat diet-induced metabolic alterations in male mice. *Endocrinology* 2016; 157: 648–65.
- 10 McInnes KJ, Smith LB, Hunger NI, Saunders PT, Andrew R, *et al*. Deletion of the androgen receptor in adipose tissue in male mice elevates retinol binding protein 4 and reveals independent effects on visceral fat mass and on glucose homeostasis. *Diabetes* 2012; 61: 1072–81.
- 11 Lin HY, Yu IC, Wang RS, Chen YT, Liu NC, *et al*. Increased hepatic steatosis and insulin resistance in mice lacking hepatic androgen receptor. *Hepatology* 2008; 47: 1924–35.
- 12 Ophoff J, Van Proeyen K, Callewaert F, De Gendt K, De Bock K, *et al*. Androgen signaling in myocytes contributes to the maintenance of muscle mass and fiber type regulation but not to muscle strength or fatigue. *Endocrinology* 2009; 150: 3558–66.
- 13 Bourlier V, Zakaroff-Girard A, Miranville A, De Barros S, Maumus M, *et al*. Remodeling phenotype of human subcutaneous adipose tissue macrophages. *Circulation* 2008; 117: 806–15.
- 14 Gerriets VA, MacIver NJ. Role of T cells in malnutrition and obesity. *Front Immunol* 2014; 5: 379.
- 15 Kanda H, Tateya S, Tamori Y, Kotani K, Hiasa K, *et al*. MCP-1 contributes to macrophage infiltration into adipose tissue, insulin resistance, and hepatic steatosis in obesity. *J Clin Invest* 2006; 116: 1494–505.
- 16 Lynch L, Nowak M, Varghese B, Clark J, Hogan AE, *et al*. Adipose tissue invariant NKT cells protect against diet-induced obesity and metabolic disorder through regulatory cytokine production. *Immunity* 2012; 37: 574–87.
- 17 Rubinow KB, Wang S, den Hartigh LJ, Subramanian S, Morton GJ, *et al*. Hematopoietic androgen receptor deficiency promotes visceral fat deposition in male mice without impairing glucose homeostasis. *Andrology* 2015; 3: 787–96.
- 18 Trigunaita A, Dimo J, Jørgensen TN. Suppressive effects of androgens on the immune system. *Cell Immunol* 2015; 294: 87–94.
- 19 De Taeye BM, Novitskaya T, McGuinness OP, Gleaves L, Medda M, *et al*. Macrophage TNF- $\alpha$  contributes to insulin resistance and hepatic steatosis in diet-induced obesity. *Am J Physiol Endocrinol Metab* 2007; 293: E713–25.
- 20 Odegaard JI, Chawla A. Mechanisms of macrophage activation in obesity-induced insulin resistance. *Nat Clin Pract Endocrinol Metab* 2008; 4: 619–26.
- 21 Lu C, Kumar PA, Fan Y, Sperling MA, Menon RK. A novel effect of growth hormone on macrophage modulates macrophage-dependent adipocyte differentiation. *Endocrinology* 2010; 151: 2189–99.
- 22 Kranendonk ME, Visseren FL, van Balkom BW, Nolte-t Hoen EN, van Herwaarden JA, *et al*. Human adipocyte extracellular vesicles in reciprocal signaling between adipocytes and macrophages. *Obesity* 2014; 22: 2216–23.
- 23 Chazenbalk G, Bertolotto C, Heneidi S, Jumabay M, Trivax B, *et al*. Novel pathway of adipogenesis through cross-talk between adipose tissue macrophages, adipose stem cells and adipocytes: evidence of cell plasticity. *PLoS One* 2011; 6: e17834.
- 24 Figueroa F, Davicino R, Micalizzi B, Oliveros L, Forneris M. Macrophage secretions modulate the steroidogenesis of polycystic ovary in rats: effect of testosterone on macrophage pro-inflammatory cytokines. *Life Sci* 2012; 90: 733–9.
- 25 Gilliver SC, Ashworth JJ, Mills SJ, Hardman MJ, Ashcroft GS. Androgens modulate the inflammatory response during acute wound healing. *J Cell Sci* 2006; 119: 722–32.
- 26 Lai JJ, Lai KP, Chuang KH, Chang P, Yu IC, *et al*. Monocyte/macrophage androgen receptor suppresses cutaneous wound healing in mice by enhancing local TNF- $\alpha$  expression. *J Clin Invest* 2009; 119: 3739–51.
- 27 Chakraborty P, William Buaas F, Sharma M, Smith BE, Greenlee AR, *et al*. Androgen-dependent sertoli cell tight junction remodeling is mediated by multiple tight junction components. *Mol Endocrinol* 2014; 28: 1055–72.

- 28 Clausen BE, Burkhardt C, Reith W, Renkawitz R, Förster I. Conditional gene targeting in macrophages and granulocytes using LysMcre mice. *Transgenic Res* 1999; 8: 265–77.
- 29 Kaiyala KJ, Morton GJ, Leroux BG, Ogimoto K, Wisse B, *et al*. Identification of body fat mass as a major determinant of metabolic rate in mice. *Diabetes* 2010; 59: 1657–66.
- 30 Folch J, Lees M, Sloane Stanley GH. A simple method for the isolation and purification of total lipides from animal tissues. *J Biol Chem* 1957; 226: 497–509.
- 31 Subramanian S, Goodspeed L, Wang S, Kim J, Zeng L, *et al*. Dietary cholesterol exacerbates hepatic steatosis and inflammation in obese LDL receptor-deficient mice. *J Lipid Res* 2011; 52: 1626–35.
- 32 Kaiyala KJ, Morton GJ, Thaler JP, Meek TH, Tylee T, *et al*. Acutely decreased thermoregulatory energy expenditure or decreased activity energy expenditure both acutely reduce food intake in mice. *PLoS One* 2012; 7: e41473.
- 33 Weir JB. New methods for calculating metabolic rate with special reference to protein metabolism. *J Physiol* 1949; 109: 1–9.
- 34 Rubinow KB, Wall VZ, Nelson J, Mar D, Bomsztyk K, *et al*. Acyl-CoA synthetase 1 is induced by gram-negative bacteria and lipopolysaccharide and is required for phospholipid turnover in stimulated macrophages. *J Biol Chem* 2013; 288: 9957–70.
- 35 Jelinek D, Castillo JJ, Arora SL, Richardson LM, Garver WS. A high-fat diet supplemented with fish oil improves metabolic features associated with type 2 diabetes. *Nutrition* 2013; 29: 1159–65.
- 36 Day SD, Enos RT, McClellan JL, Steiner JL, Velázquez KT, *et al*. Linking inflammation to tumorigenesis in a mouse model of high-fat-diet-enhanced colon cancer. *Cytokine* 2013; 64: 454–62.
- 37 Chang C, Yeh S, Lee SO, Chang TM. Androgen receptor (AR) pathophysiological roles in androgen-related diseases in skin, bone/muscle, metabolic syndrome and neuron/immune systems: lessons learned from mice lacking AR in specific cells. *Nucl Recept Signal* 2013; 11: e001.
- 38 Rana K, Fam BC, Clarke MV, Pang TP, Zajac JD, *et al*. Increased adiposity in DNA binding-dependent androgen receptor knockout male mice associated with decreased voluntary activity and not insulin resistance. *Am J Physiol Endocrinol Metab* 2011; 301: E767–78.
- 39 Yu IC, Lin HY, Liu NC, Sparks JD, Yeh S, *et al*. Neuronal androgen receptor regulates insulin sensitivity via suppression of hypothalamic NF- $\kappa$ B-mediated PTP1B expression. *Diabetes* 2013; 62: 411–23.
- 40 Ribas V, Drew BG, Le JA, Soleymani T, Daraei P, *et al*. Myeloid-specific estrogen receptor alpha deficiency impairs metabolic homeostasis and accelerates atherosclerotic lesion development. *Proc Natl Acad Sci U S A* 2011; 108: 16457–62.
- 41 Yanase T, Fan W, Kyoya K, Min L, Takayanagi R, *et al*. Androgens and metabolic syndrome: lessons from androgen receptor knock out (ARKO) mice. *J Steroid Biochem Mol Biol* 2008; 109: 254–7.
- 42 Qiu Y, Yanase T, Hu H, Tanaka T, Nishi Y, *et al*. Dihydrotestosterone suppresses foam cell formation and attenuates atherosclerosis development. *Endocrinology* 2010; 151: 3307–16.
- 43 Huang CK, Pang H, Wang L, Niu Y, Luo J, *et al*. New therapy via targeting androgen receptor in monocytes/macrophages to battle atherosclerosis. *Hypertension* 2014; 63: 1345–53.
- 44 Huang CK, Luo J, Lai KP, Wang R, Pang H, *et al*. Androgen receptor promotes abdominal aortic aneurysm development via modulating inflammatory interleukin-1 $\alpha$  and transforming growth factor- $\beta$ 1 expression. *Hypertension* 2015; 66: 881–91.
- 45 Vannella KM, Barron L, Borthwick LA, Kindrachuk KN, Narasimhan PB, *et al*. Incomplete deletion of IL-4R $\alpha$  by LysM (Cre) reveals distinct subsets of M2 macrophages controlling inflammation and fibrosis in chronic schistosomiasis. *PLoS Pathog* 2014; 10: e1004372.

This is an open access journal, and articles are distributed under the terms of the Creative Commons Attribution-NonCommercial-ShareAlike 4.0 License, which allows others to remix, tweak, and build upon the work non-commercially, as long as appropriate credit is given and the new creations are licensed under the identical terms.

©The Author(s)(2017)